Chemical Physics Letters 685 (2017) 251–258

Contents lists available at ScienceDirect

Chemical Physics Letters

journal homepage: www.elsevier.com/locate/cplett

Research paper

Strengthening of hydrogen bonding with the push-pull effect ☆

Yunwen Tao [a], Wenli Zou [b], Elfi Kraka [a,*]

[a] Computational and Theoretical Chemistry Group (CATCO), Department of Chemistry, Southern Methodist University, 3215 Daniel Avenue, Dallas, TX 75275-0314, United States
[b] Institute of Modern Physics, Northwest University, Xi'an, Shaanxi 710069, PR China

ARTICLE INFO

Article history:
Received 13 June 2017
In final form 26 July 2017
Available online 27 July 2017

ABSTRACT

Theoretical studies of hydrogen-bonding based on cluster models tend to overlook the peripheral monomers which are influential. By revisiting thirteen hydrogen-bonded complexes of H_2O, HF and NH_3, the "push-pull" effect is identified as a general mechanism that strengthens a hydrogen bond. Enhanced $Lp(X) \rightarrow \sigma^*(X'-H)$ charge transfer is proved to be the core of the "push-pull" effect. The charge transfer can convert an electrostatic hydrogen bond into a covalent hydrogen bond.

1. Introduction

Hydrogen bonding (H-bonding) is one of the most important intermolecular forces found in condensed phases, especially in the case of liquid water. It decides on various macroscopic properties including density, boiling point and melting point. In the recent years, various quantum chemical studies attempted to look into the H-bonding by simulating real systems with the help of cluster models consisting of 2–20 monomers [1–11]. Various computational methods have been used for the analysis of H-bonds including binding energy calculation [1,6–8,10], energy decomposition analyses [12] or the quantum theory of atoms in molecules and the natural bond orbital (NBO) analysis [13]. However, a deeper analysis of how peripheral monomers around a dimer influence the targeted H-bond is often missing.

Experimental studies on the OH stretching frequency shift in small water clusters, supported by DFT calculations, have suggested that the formation and strength of a particular H-bond is influenced by cooperative effects from peripheral H-bonds [14,15]. However, a caveat is appropriate. Experimentally or theoretically derived normal vibrational modes and force constants are delocalized because of electronic and mass-coupling [16]. Therefore, are not suited as direct measure of bond strength [17]. We present in this work a reliable descriptor of the intrinsic H-bond strength based on local vibrational modes, first introduced by Konkoli and Cremer [16,18]. These local modes have been proved to be the local equivalent of the delocalized normal vibrational modes via an adiabatic connection scheme (ACS), in which a one-to-one relationship has been proved between $3N-L$ normal modes and a non-redundant set of $3N-L$ local modes (N: number of atoms; L: number of translations and rotations) [18]. The local stretching force constant k^a is the appropriate tool to describe the intrinsic bond strength of any chemical bonding situation [19,17], including non-covalent bonding [20,21] like hydrogen bonds [22,23]. Since k^a is directly related to the electronic structure of a molecule, it absorbs any neighboring influences on the bond in question, such as cooperative effects [23].

In this work, we have studied thirteen clusters made up of monomers of H_2O, HF and NH_3 molecules. A new and generally applicable mechanism which we name as *push-pull* effect is identified to strengthen H-bonds. This push-pull effect can have a strong impact on the H-bonding mechanism in several cases. The objectives of this work are to answer the following questions. (i) What is push-pull effect in H-bonding? (ii) How can the push-pull effect strengthen a H-bond? (iii) How is the push-pull effect related to the charge transfer from the H-bond acceptor to the H-bond donor? (iv) To what extent can the push-pull effect change the nature of a H-bond with regard to its covalent or electrostatic character?

The computational methods used in this work are described in the second section. The third section presents the results and discussion, while conclusions are made in the final section.

2. Computational methods

Optimized geometries of all clusters investigated in this work (see Fig. 1) and their vibrational frequencies as well as normal modes were calculated using the ωB97X-D density functional. This functional was chosen because it describes non-covalent interactions in a reliable way taking care of dispersion and other van der Waals interactions [24–27]. Pople's triple zeta basis set 6-311 ++G(d,p) with diffuse functions for O, F, N and H atoms was used.

☆ In Memoriam of Dieter Cremer.

* Corresponding author.
E-mail address: ekraka@smu.edu (E. Kraka).

http://dx.doi.org/10.1016/j.cplett.2017.07.065
0009-2614/

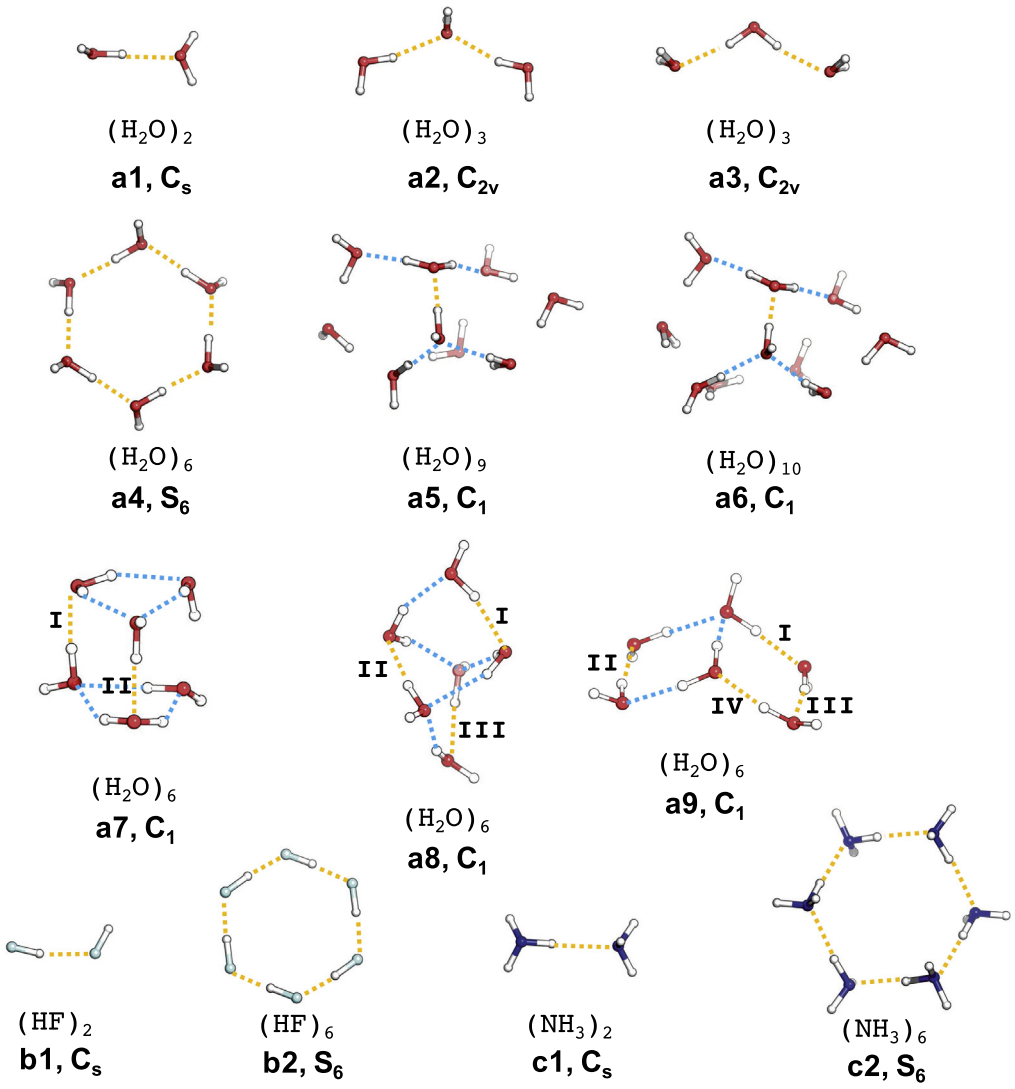

Fig. 1. Schematic presentation of the geometries of cluster **a1**–**c2**. Red, cyan, blue and white spheres stand for oxygen, fluorine, nitrogen and hydrogen atoms respectively. Yellow dashed lines indicate the hydrogen bonds described in Table 1. Blue dashed lines in **a5**–**a9** are used to represent the peripheral hydrogen bonds responsible for push-pull mechanism. The components, labels and symmetry of each cluster is also given. (For interpretation of the references to color in this figure legend, the reader is referred to the web version of this article.)

This basis set provides an accurate description for these molecular clusters [28–30]. The DFT calculations were conducted using a pruned (99,590) UltraFine integration grid [31,32] and the geometry optimization was imposed with a tight convergence criterion to guarantee the accurate calculation of the Hessian matrix which was used for adiabatic local mode analysis.

The geometries of two additional small water clusters (hexamer and tetramer) shown in Fig. 2 were constructed based on the geometry of water dimer[1] in **a1**, constrained by C_s symmetry.

The electron density was calculated at the ωB97X-D/6-311G++(d,p) level of theory. The charge transfer was analyzed based on calculated NPA charges [33,34].

The intrinsic bond strength of the H-bond was determined by the local H-bond stretching force constant k^a [22,17] derived from the corresponding local vibrational mode [16].

The covalent character of the H-bonds was estimated via the calculation of the delocalization energy ΔE_{del}, which can be understood as the stabilization energy due to the charge transfer from one or more (if present) lone pair orbital(s) of the X atom of the hydrogen bond acceptor to a σ^* antibonding X′-H orbital of the hydrogen bond donor through the overlap between the two orbitals. The amplitude of ΔE_{del} was characterized for a given X...X′-H interaction by a second order perturbation theory analysis of the Fock matrix in the NBO basis [34].

The nature of the H-bond was further characterized by the local energy density H_b at the (3,-1) bond critical point $\mathbf{r_b}$(BCP) [35,36]. The Cremer-Kraka criteria were applied to quantitatively identify the covalent bonding character: (i) A BCP and zero-flux surface must exist between the two atoms, for which chemical bonding is expected (*necessary condition*). (ii) The local energy density H_b must be less than zero in the case of covalent bonding (*sufficient condition*). Positive values of H_b indicates that the bond in question is dominated by electrostatic interactions [37]. This descriptor has been extensively used in the studies of chemical bonds to determine whether a bond is covalent or non-covalent [38,39], including pnicogen bonds, [21] halogen bonds, [20] and hydrogen bonds [1,22,23].

Apart from characterizing the charge transfer within the H-bond dimer using the NBO analysis, we also calculated the difference density distribution $\Delta\rho(A\ldots B,\mathbf{r}) = \rho(AB,\mathbf{r}) - (\rho(A,\mathbf{r}) + \rho(B,\mathbf{r}))$[40], to describe the formation of the complex *AB* where a hydrogen bond is found between monomers *A* and *B* with regard

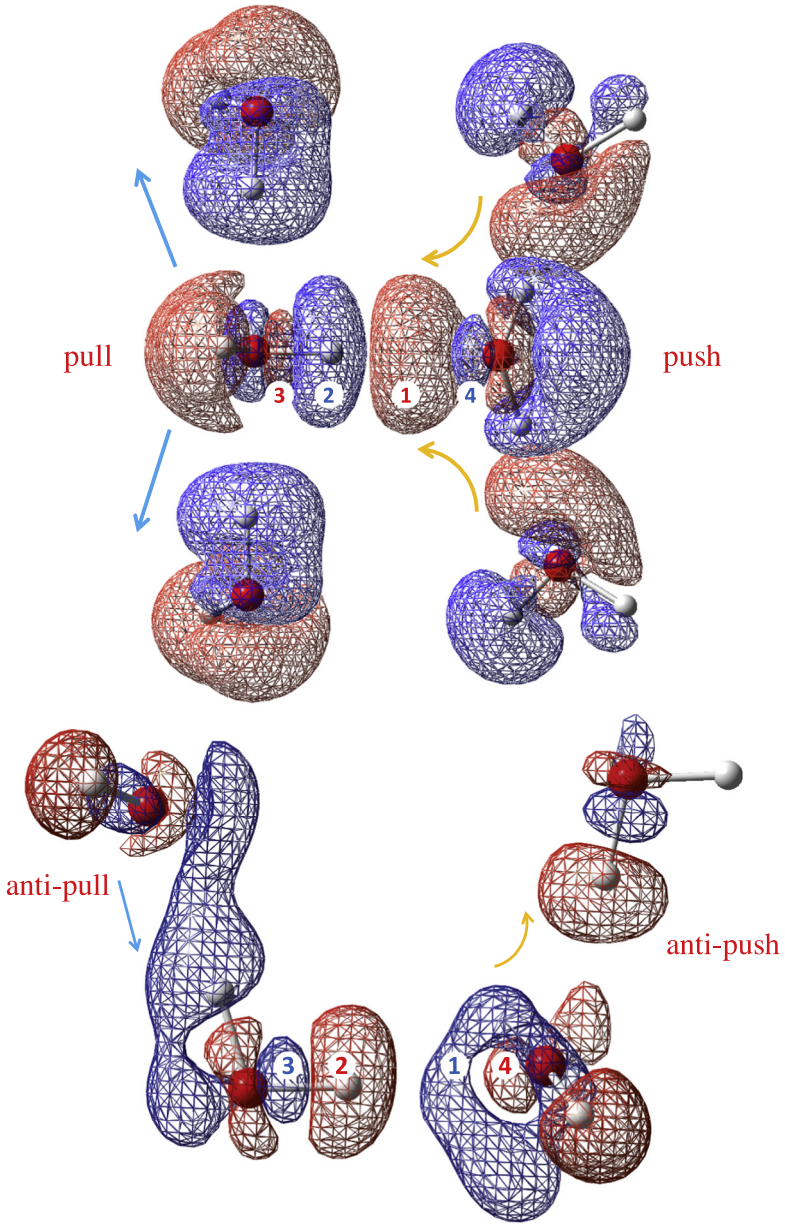

Fig. 2. Electron difference density distribution $\Delta\rho$ shown as the $\pm$0.0002 e/Bohr^3 isosurface. Blue surface indicates electron depletion, red is increased electron density region. Top: 20–02 type H-bond in the center with a push-pull effect. Bottom: 01–10 type H-bond in the bottom with an antipush-antipull effect. (For interpretation of the references to color in this figure legend, the reader is referred to the web version of this article.)

to the change of the electron density distribution. The push-pull effect caused by peripheral molecules can be made visible with the help of the above formula. Besides taking only one monomer as the H-bond donor(D) and one as acceptor(A) for the hydrogen bond in question, we defined a generalized H-bond donor (D^*) and acceptor (A^*) which include D and A respectively but can have more than one monomer. Within the complex of D^* or A^*, the monomers are connected via peripheral hydrogen bonds, which need to be distinguished from the targeted H-bond in the center. In this way, the influence of these peripheral monomers on the central DA dimer complex in H-bonding can be assessed from $\Delta\rho(push-pull) = \Delta\rho(D^*\ldots A^*,\mathbf{r}) - \Delta\rho(D\ldots A,\mathbf{r}) = \rho(D^*A^*,\mathbf{r}) - \rho(D^*,\mathbf{r}) - \rho(A^*,\mathbf{r}) - \rho(DA,\mathbf{r}) + \rho(D,\mathbf{r}) + \rho(A,\mathbf{r})$ [23]. As an example, the molecular cluster **a4** in Fig. 4 has its polarization effect on the bottom hydrogen bond arising from the four peripheral waters visualized accordingly.

All vibrational modes as well as the local mode analysis were carried out with the program package COLOGNE2017 [41], whereas for the DFT calculations, the program package Guassian09 [42] was used. Difference densities and NBO orbitals were plotted with the Multiwfn program [43].

3. Results and discussion

Fig. 1 summarizes the 13 molecular clusters investigated in this work labeled with **a1**–**a9**, [44] **b1**–**b2** and **c1**–**c2**. In each cluster, we have one target H-bond in question with regard to the push-pull effect shown in yellow dashed lines. For clusters with high symmetry, we have several symmetry equivalent target H-bonds [3–5,2]. Properties of the target H-bond are summarized in Table 1 including the notation of H-bond type, bond length *R*, local

Table 1
Properties of the target H-bond of clusters **a1**–**a9**, **b1**–**b2** and **c1**–**c2**.[a]

Cluster #	Complex	Type	R	k^a	ΔE_{del}	H_b
a1	$(H_2O)_2$	00–00	1.9158	0.199	9.67	+0.002299
a2	$(H_2O)_3$	01–00	1.9659	0.168	8.15	+0.002352
a3	$(H_2O)_3$	00–10	1.9666	0.165	8.11	+0.002312
a9-II	$(H_2O)_6$	10–01	1.7969	0.265	16.86	+0.000383
a4	$(H_2O)_6$	10–01	1.7261	0.359	22.51	−0.001673
a9-III	$(H_2O)_6$	10–01	1.7156	0.344	24.29	−0.002485
a8-I	$(H_2O)_6$	10–02	1.8080	0.251	18.05	−0.000213
a9-IV	$(H_2O)_6$	10–02	1.7161	0.344	25.13	−0.002759
a8-III	$(H_2O)_6$	20–01	1.7544	0.297	20.52	−0.001022
a9-I	$(H_2O)_6$	20–01	1.6997	0.328	25.98	−0.003107
a7-II	$(H_2O)_6$	20–02	1.7530	0.311	22.17	−0.001500
a8-II	$(H_2O)_6$	20–02	1.6831	0.328	30.71	−0.005091
a7-I	$(H_2O)_6$	20–02	1.6692	0.366	32.17	−0.005725
a5	$(H_2O)_9$	20–02	1.6106	0.395	38.67	−0.008851
a6	$(H_2O)_{10}$	20–02	1.6103	0.399	38.57	−0.008770
b1	$(HF)_2$	00–00	1.8277	0.182	8.38	+0.002529
b2	$(HF)_6$	10–01	1.5524	0.420	30.93	−0.004162
c1	$(NH_3)_2$	00–00	2.2080	0.117	6.40	+0.001782
c2	$(NH_3)_6$	10–01	2.0847	0.178	11.83	+0.001361

[a] Hydrogen bond length R in Å, local stretching force constant k^a in mdyn/Å, delocalization energy $\Delta E_{del} = \Delta E_{lp(X)\rightarrow\sigma^*(X'-H)}$ in kcal/mol (X = X′ = O, F or N), local energy density H_b in Hartree/Bohr^3.

stretching force constant k^a, the delocalization energy ΔE_{del} and local energy density H_b. Fig. 2 illustrates the push-pull effect using the electron density difference (EDD) of the H-bond in water. The opposite effect, coined as antipush-antipull effect is also shown. In Fig. 3, the NBOs responsible for the dominating $lp(X) \rightarrow \sigma^*(X'-H)$ charge transfer leading to stabilization are shown for the H-bond donor and also acceptor within H-bond dimer for **a1**, **b1** and **c1**. In Fig. 4, the push-pull effect for a specific H-bond is visualized via electron density difference maps for the hexamer rings of H_2O, HF and NH_3(clusters **a4**, **b2** and **c2** respectively).

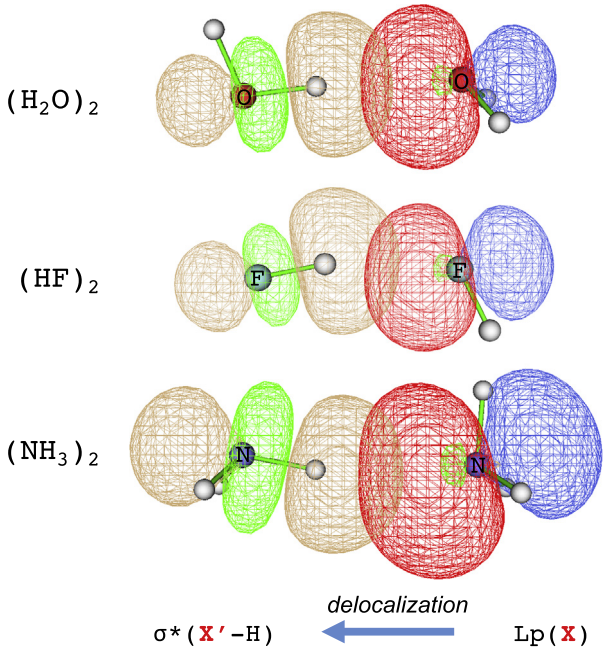

Fig. 3. Charge transfer in the formation of a hydrogen bond implies electron delocalization of lone pair electrons in Lp(X) orbital (red and blue lobes on the right as H-bond acceptor) into the unoccupied σ^*(X′-H) antibonding orbital (brown and green lobes on the left as H-bond donor). For H_2O and HF, only one of the lone pair orbitals is shown here as the dominating one with regard to ΔE_{del}. (For interpretation of the references to color in this figure legend, the reader is referred to the web version of this article.)

3.1. Different types of H-bonds

We showed in previous work [23] how the properties of a H-bond donor and acceptor are affected by the surrounding molecules. We used a 4-digit notation ($i_a j_d - k_a l_d$) in order to distinguish between different kinds of H-bonding. In this work, we will use the same notation.

We use 00–00 to denote the H-bond in a dimer structure. If the donor water accepts 1 H-bond from other water molecules, we add 1 to i_a and if the donor water donates 1 extra H-bond to a peripheral water which needs to be distinguished from the acceptor water of 00–00 H-bond, we add 1 to j_d. This rule also applies to the acceptor water as the ($i_a j_d$) part is for the donor while acceptor water is determined by the ($k_a l_d$) part.

We have found in our previous studies on the water clusters that for some specific types of H-bond, the intrinsic H-bond strength based on local stretching force constant k^a is remarkably higher or lower than for some other types [23]. Similar observations were also made in this work (see Table 1).

3.2. Definition of the push-pull effect

In order to define the push-pull effect in H-bonding, three major ingredients are needed, including (i) the way how the H-bond donor and acceptor molecules interact with peripheral molecules via peripheral H-bonding, (ii) the electron density difference $\Delta\rho$ (*push-pull*) showing the influence of peripheral molecules on the central H-bond contained within a dimer structure and (iii) the intrinsic H-bond strength characterized by k^a. This definition of the "push-pull" effect must not be confused with the originally use of the term "push-pull" effect proposed by Kleinpeter [45] for the description of covalent π bonding.

If a specific H-bond of a molecular complex AB connected via H-bonding is to be studied, it is insufficient if just to focus on the A and B monomer. It is necessary to include those molecules that directly interact with the donor and acceptor as these peripheral molecules may lead to a significant change in the electronic structure of the H-bond in question via polarization.

For the $(H_2O)_6$ cluster shown on top of Fig. 2, the H-bond in the central dimer can be classified as 20–02 type, namely the H-bond donor water on the left hand side accepts 2 external H-bonds while the H-bond acceptor on the right hand side donates 2 external

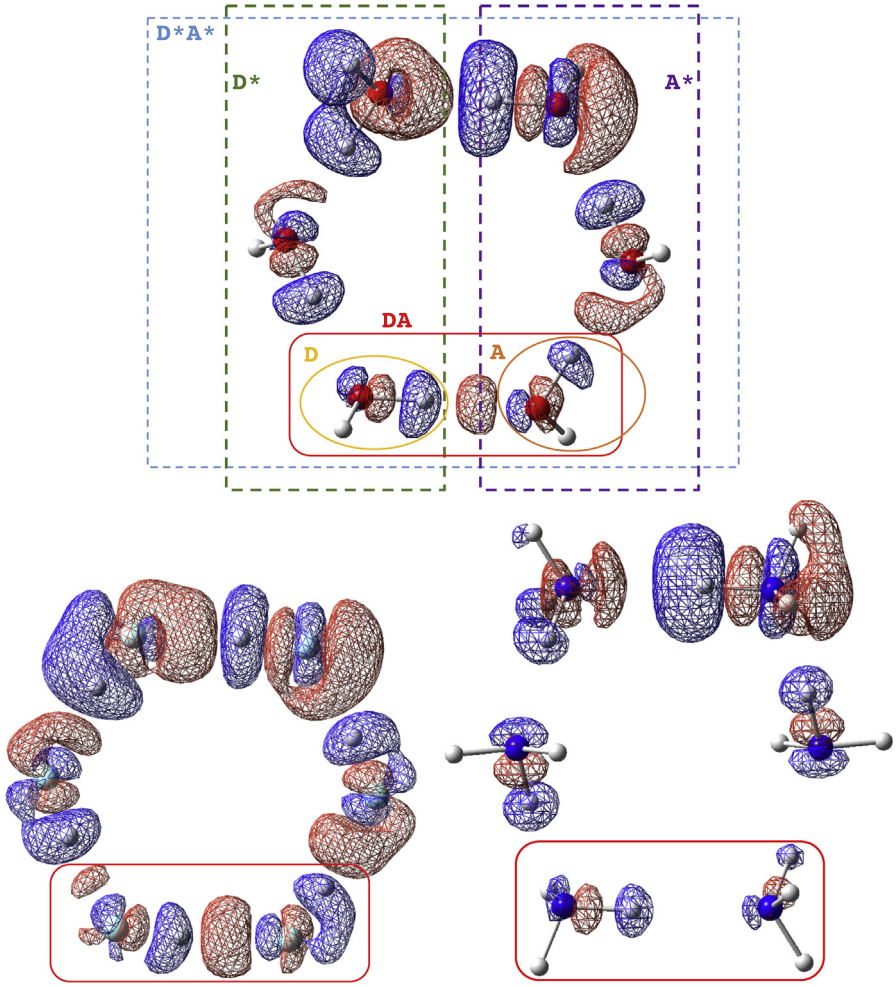

Fig. 4. Electron density difference maps of $\Delta\rho(push - pull)$ for hexamer rings. The target H-bond is identified by the red box. Upper: **a4**; Lower left: **b2**; Lower right: **c2**. Red mesh surfaces depict a density increase while blue mesh surfaces for density decrease. Isovalue for surfaces is ±0.001 e/Bohr^3. (For interpretation of the references to color in this figure legend, the reader is referred to the web version of this article.)

H-bonds to other water molecules. The electron density difference distribution is calculated by subtracting from the density of the whole hexamer that of the trimer on the donor and acceptor side as well as that of the dimer in the center then adding that of the donor and acceptor water of 20–02 H-bond (short notation: 6–2 × 3–2 + 1 + 1). This EDD map shows how the 4 peripheral water molecules polarize the H-bond in the central water dimer. On the acceptor side, these two peripheral water molecules which accept H-bonds have their lone pairs pointing to this acceptor water. These lone pairs increase the electron density distribution in the central H-bond region by polarization(labeled as ① in red color). We name this polarization as "push". On the donor side of 20–02 H-bond, two additional water molecules donating extra H-bonds further polarize the electron density. For this 20–02 H-bond, the donor OH covalent bond has a decreased density around the H atom(② in blue color), then it has an increased density towards the donor O atom (③ in red color). These two peripheral waters withdraw electron density from the central H-bond region, so we say they can "pull" electron density. When we combine the polarization effect both on the acceptor side and on the donor side, the comprehensive effect is summarized as "push-pull" effect.

We note that between the donor oxygen and the acceptor oxygen within this 20–02 H-bond, there is a region in which electron density is decreased (④ in blue color), which we will discuss below.

For the assurance of the validity of the definition of the push-pull effect, we checked other water clusters, for example the tetramer shown on the bottom of Fig. 2. Here we reverted all polarization effect on the central targeted H-bond in 20–02 simply by changing it into the 01–10 H-bonding situation where the donor water accepts no H-bonds but needs to donate 1 extra H-bond and the acceptor water accepts 1 extra H-bond while donating no H-bonds. As a result, the acceptor water has to direct its second lone pair to the water from which it accepts another H-bond, so the central H-bond region has a decreased electron density (① in blue color). Such a polarization can be coined as the opposite to "push" as "anti-push" effect. On the other hand, the water to which the donor water's extra H-bond points has its lone pair electrons oriented to one of the OH bonds of the donor water. This leads to the density increase in region ② and decrease in region ③. Such a distribution pattern is opposite to its counterpart in 20–02, thus we call this "anti-pull" effect.

3.3. Intrinsic H-bond strength, change transfer and covalency

Table 1 provides a summary of 15 different H-bonds found in 9 clusters of H_2O, in addition to 4 H-bonds in clusters of HF and NH_3.

Taking the 00–00 H-bond in the dimer **a1** as the reference, we find that the 01–00 and 00–10 H-bonds in **a2** and **a3** resulting from an anti-pull and anti-push effect respectively, are characterized by

longer bond lengths, decreased intrinsic bond strengths, smaller delocalization energies and more positive H_b values. In contrast, the other H-bonds of the type X0-0Y (X,Y > 0) for which the push-pull effect plays a dominant role have shorter and stronger bonds. The charge transfer is more pronounced and they are of covalent character, as reflected by negative H_b values. There is one exception, the relatively weak 10–01 H-bond in **a9-II** has a small positive H_b value, see Table 1.

While all of the H-bonds supported by peripheral push- and pull H-bonds are stronger than the 00–00 H-bond without any push–pull effect, the H-bonds of type 10–02, 20–01 or 20–02 are not necessarily stronger than the 10–01 H-bonds, even though they seem to be strengthened by a larger number of the push-pull molecules. The reason for this observation is that the magnitude of the push and pull effect varies from one H-bond to another. A closer examination of the results reveals that stronger pushing and pulling H-bonds can render a significant increase in H-bond strength, while weaker pushing and pulling H-bonds offer limited increase of intrinsic bond strength. The strongest H-bonds with local stretching force constant k^a values up to 0.39 mdyn/Å are found for the 20–02 type. This implies that there exists an upper bound with regard to the intrinsic bond strength for each push-pull type, given that the number of H-bonds studied is large enough to cover as many H-bonding possibilities as possible.

The NBO analysis carried out by Reed et al. [46] suggests that charge transfer plays an important role in the formation of H-bonds. In our work, the results of the NBO analysis show that the most stabilizing factor within a H-bond dimer complex is the interaction between the lone pair orbital(s) of the H-bond acceptor $Lp(X)$ and the σ^* anti-bonding orbital of the $X'-H$ covalent bond with the H-bond donor pointing to the acceptor atom X. Fig. 3 shows the shape of the NBOs of $Lp(X)$ and $\sigma^*(X'-H)$ from which the dominating stabilization in H-bonding is established. These NBO plots are consistent for the dimer of H_2O, HF and NH_3. Furthermore, if one takes a closer look at the space between atoms X and X', in total 4 lobes can be identified. The four different regions, labeled 1–4 in Fig. 2 directly match the four lobes shown in Fig. 3 from left to right as green-③, brown-②, red-① and then green-④.

It is interesting to note that for H-bonds in water, the variation in the delocalization energy ΔE_{del} characterizing the charge transfer from $Lp(X)$ to $\sigma^*(X'-H)$ is consistent with the change of local stretching force constant k^a; the more charge transfer a H-bond has, the stronger is this H-bond, see Table 1. However, there are two expections, complexes **a9-II** and **a8-I**. They possess the weakest H-bonds, (k^a values of 0.265 and 0.251 mdyn/Å respectively) compared to the other push-pull H-bonds, (k^a values in the range of 0.297–0.399 mdyn/Å). The H_b values of these two H-bonds are less negative than for the other push-pull H-bonds. The 10–01 H-bond in **a9-II** is a borderline case with a small positive H_b value. Therefore, according to the Cremer-Kraka criteria [37,38], this H-bond is dominated by classical electrostatic interactions.

The electrostatic interaction in H-bonding has been a controversial topic since the first recognition of the H-bond phenomenon [47]. For example, Weinhold and co-workers proposed that the driving force of the formation of a H-bond is charge transfer, while classical electrostatic forces as well as dispersion forces are of minor importance [48]. They even discussed the "anti-electrostatic hydrogen bond" [49], in which classical electrostatic forces are destabilizing and only charge transfer plays the leading role.

We clearly identify the H-bonds in **a1**–**a3** as dominated by electrostatic interactions rather than by charge transfer. (i) They are characterized by positive H_b values, indicating the increased weight of electrostatic interactions over covalent character (see Table 1); (ii) The charge transfer is diminished (characterized by decreased ΔE_{del} values) via the anti-push or anti-pull effect. For the 10–01 H-bond in **a9-II**, although the charge transfer is increased compared to the H-bond in water dimer, the covalent contribution from charge transfer is still not as important as the electrostatic forces. So that the local energy density remains positive, but its value is less positive than that for the 00–00 H-bond. When the delocalization energy is increased to 18.05 kcal/mol for the H-bond in **a8-I**, the local energy density immediately turns negative, indicating the dominance of charge transfer over classical electrostatic forces. The other push-pull H-bonds of water investigated in this work are of covalent nature as indicated by negative H_b values and dominated by charge transfer, as reflected by the data in Table 1. It is interesting to note that the local energy density H_b increases with increasing delocalization energy ΔE_{del}, and no exceptions are identified. This correlation (see Fig. 1 in Supporting Information) suggests that both, the local energy density H_b and the delocalization energy ΔE_{del} are reliable descriptors of charge transfer/covalency; where the local energy density in addition allows to distinguish between covalent and the electrostatic interaction.

Apart from the H-bonds in water, we have also studied the H-bonds in the HF and NH_3 clusters with regard to the push-pull effect. The dimer structures **a1**, **b1** and **c1** can be directly compared as well as the ring hexamer structures **a4**, **b2** and **c2** respectively for H_2O, HF and NH_3. The result shows that the H-bonding in the case of HF is most sensitive to the push-pull effect as it has the largest increase in bond strength and charge transfer. Furthermore, it adapts more covalent character when it is changed from 00–00 type to 10–01 type, in the same way as this happens for H_2O. In contrast the H-bonding in the case of NH_3 is least responsive to the push-pull effect, as it has the least increase in the local stretching force constant and the delocalization energy. It remains dominated by the classical electrostatic forces regardless of pushing and pulling H-bond neighbors. This is illustrated by the electron density difference plots for the hexamer rings of **a4**, **b2** and **c2** shown in Fig. 4. The HF hexamer ring **b2** has the largest electron density accumulation region, while such a region cannot be found in the case of NH_3 hexamer ring **c2**. These observations can be explained by the fact that the HF molecule has up to 3 lone pairs while H_2O and NH_3 has only 2 and 1 lone pairs respectively, so that HF molecule shows the most response to the push-pull effect in H-bonding.

4. Conclusions

In this work, we have for the first time defined the concept of the push-pull effect in H-bonds and examined this effect for 13 molecular complexes. This investigation has led to a series of interesting results.

(1) The characteristic EDD map of $\Delta\rho(push-pull)$ shows that the push-pull effect is a real and observable change in the electronic structure in H-bonding. The push-pull is a general effect and exists in H-bonded clusters constituted by monomers of the same type.
(2) The intrinsic H-bond strength is directly related to the push-pull effect. The larger is the push-pull effect, the larger is the H-bond strengthening. A H-bond can be weakened if it is under the influence of the anti-pull or the anti-push effect. The mixing of push-pull effect and the antipush-antipull effect may lead to an interesting competition and a variety of H-bond possibilities. This will be part of a future investigation.

(3) The strong correlation between the NBO diagrams ($Lp(X)$ and $\sigma^*(X'-H)$) and the $\Delta\rho(push-pull)$ EDD maps with regard to the central H-bond region indicates the origin of push-pull effect is the enhanced charge transfer which is responsible for the H-bonding stabilization. Furthermore, the more charge transfer a H-bond has, ideally the stronger this H-bond can be.

(4) Among the clusters studied in this work, the HF clusters are more responsive to the push-pull effect than H_2O and NH_3 clusters. H-bonds in NH_3 clusters are not influenced significantly with regard to their intrinsic bond strength and bonding nature. Similar observations are to be expected for the clusters of H_2S, HCl and PH_3. Work is in progress to demonstrate this.

(5) The push-pull effect can increase the covalent character of a H-bond via enhanced charge transfer. Increased covalency can change the nature of a H-bond depending on whether the covalent character can override the electrostatic character. If so, the H-bond will be more like a covalent bond although H-bonds are generally weaker than normal covalent bonds.

(6) The H-bonds in the dimer structure of H_2O, HF and NH_3 are dominated by electrostatic force. However, one can find H-bonds which are dominated by covalent character in the clusters of H_2O or HF.

(7) Contrary to Stones' claim that "it is a serious error to use NBO method in analyzing intermolecular interactions" [50], apparently the NBO analysis remains still a powerful tool for H-bonding studies in two ways: (i) the NBO diagrams shown in Fig. 3 is closely related to the EDD maps characterizing $\Delta\rho(push-pull)$; (ii) the variation in the quantitative measurement of the amplitude in charge transfer $\Delta E_{lp(X)\rightarrow\sigma^*(X'-H)}$ is consistent with the change of k^a and H_b.

Acknowledgement

This work was financially supported by the National Science Foundation, Grant 1464906. We thank SMU for providing computational resources.

Appendix A. Supplementary material

Supplementary data associated with this article can be found, in the online version, at http://dx.doi.org/10.1016/j.cplett.2017.07.065.

References

[1] R. Kalescky, W. Zou, E. Kraka, D. Cremer, Local vibrational modes of the water dimer – comparison of theory and experiment, Chem. Phys. Lett. 554 (2012) 243–247.
[2] J. Kim, D. Majumdar, H.M. Lee, K.S. Kim, Structures and energetics of the water heptamer: comparison with the water hexamer and octamer, J. Chem. Phys. 110 (18) (1999) 9128–9134.
[3] M. Jelil, A. Abaydulla, Graph theoretical enumeration of topology-distinct structures for hydrogen fluoride clusters (HF)n (n ≤ 6), J. Chem. Phys. 143 (4) (2015) 044301.
[4] J. Friedrich, E. Perlt, M. Roatsch, C. Spickermann, B. Kirchner, Coupled cluster in condensed phase. Part i: Static quantum chemical calculations of hydrogen fluoride clusters, J. Chem. Theory Comput. 7 (4) (2011) 843–851.
[5] A. Malloum, J.J. Fifen, Z. Dhaouadi, S.G.N. Engo, N.-E. Jaidane, Structures and relative stabilities of ammonia clusters at different temperatures: DFT vs. ab initio, Phys. Chem. Chem. Phys. 17 (43) (2015) 29226–29242.
[6] R.M. Shields, B. Temelso, K.A. Archer, T.E. Morrell, G.C. Shields, Accurate predictions of water cluster formation, (H2O)n=2-10, J. Phys. Chem. A 114 (43) (2010) 11725–11737.
[7] J.C. Howard, G.S. Tschumper, Wavefunction methods for the accurate characterization of water clusters, Wiley Interdiscipl. Rev.: Comput. Mol. Sci. 4 (3) (2013) 199–224.
[8] S. Iwata, Analysis of hydrogen bond energies and hydrogen bonded networks in water clusters $(H_2O)_{20}$ and $(H_2O)_{25}$ using the charge-transfer and dispersion terms, Phys. Chem. Chem. Phys. 16 (23) (2014) 11310.
[9] I. Bakó, I. Mayer, Hierarchy of the collective effects in water clusters, J. Phys. Chem. A 120 (4) (2016) 631–638.
[10] N. Sahu, S.S. Khire, S.R. Gadre, Structures, energetics and vibrational spectra of $(H_2O)_{32}$ clusters: a journey from model potentials to correlated theory, Mol. Phys. 113 (19–20) (2015) 2970–2979.
[11] L. Huang, S.G. Lambrakos, A. Shabaev, N. Bernstein, L. Massa, Molecular analysis of water clusters: calculation of the cluster structures and vibrational spectrum using density functional theory, Compt. Rend. Chim. 18 (5) (2015) 516–524.
[12] M.J.S. Phipps, T. Fox, C.S. Tautermann, C.-K. Skylaris, Energy decomposition analysis approaches and their evaluation on prototypical protein-drug interaction patterns, Chem. Soc. Rev. 44 (10) (2015) 3177–3211.
[13] A. Shahi, E. Arunan, Hydrogen bonding, halogen bonding and lithium bonding: an atoms in molecules and natural bond orbital perspective towards conservation of total bond order, inter- and intra-molecular bonding, Phys. Chem. Chem. Phys. 16 (42) (2014) 22935–22952.
[14] K. Ohno, M. Okimura, N. Akai, Y. Katsumoto, The effect of cooperative hydrogen bonding on the OH stretching-band shift for water clusters studied by matrix-isolation infrared spectroscopy and density functional theory, Phys. Chem. Chem. Phys. 7 (16) (2005) 3005–3014.
[15] C. Tainter, Y. Ni, L.a. Shi, J. Skinner, Hydrogen bonding and OH-stretch spectroscopy in water: hexamer (cage), liquid surface, liquid, and ice, J. Phys. Chem. Lett. 4 (1) (2012) 12–17.
[16] Z. Konkoli, D. Cremer, A new way of analyzing vibrational spectra. i. Derivation of adiabatic internal modes, Int. J. Quant. Chem. 67 (1) (1998) 1–9.
[17] W. Zou, D. Cremer, C_2 in a box: determining its intrinsic bond strength for the $X^1\Sigma_g^+$ ground state, Chem. - Euro. J. 22 (12) (2016) 4087–4099.
[18] W. Zou, R. Kalescky, E. Kraka, D. Cremer, Relating normal vibrational modes to local vibrational modes with the help of an adiabatic connection scheme, J. Chem. Phys. 137 (2012) 084114.
[19] R. Kalescky, E. Kraka, D. Cremer, Identification of the strongest bonds in chemistry, J. Phys. Chem. A 117 (36) (2013) 8981–8995.
[20] V. Oliveira, E. Kraka, D. Cremer, Quantitative assessment of halogen bonding utilizing vibrational spectroscopy, Inorg. Chem. 56 (1) (2017) 488–502.
[21] D. Setiawan, E. Kraka, D. Cremer, Strength of the pnicogen bond in complexes involving group Va elements N, P, and As, J. Phys. Chem. A 119 (9) (2015) 1642–1656.
[22] M. Freindorf, E. Kraka, D. Cremer, A comprehensive analysis of hydrogen bond interactions based on local vibrational modes, Int. J. Quant. Chem. 112 (19) (2012) 3174–3187.
[23] Y. Tao, W. Zou, J. Jia, W. Li, D. Cremer, Different ways of hydrogen bonding in water - why does warm water freeze faster than cold water?, J Chem. Theory Comput. 13 (1) (2017) 55–76.
[24] K.S. Thanthiriwatte, E.G. Hohenstein, L.A. Burns, C.D. Sherrill, Assessment of the performance of DFT and DFT-D methods for describing distance dependence of hydrogen-bonded interactions, J. Chem. Theory Comput. 7 (1) (2011) 88–96.
[25] S. Kozuch, J.M.L. Martin, Halogen bonds: benchmarks and theoretical analysis, J. Chem. Theory Comput. 9 (4) (2013) 1918–1931.
[26] A. Bauzá, I. Alkorta, A. Frontera, J. Elguero, On the reliability of pure and hybrid DFT methods for the evaluation of halogen, chalcogen, and pnicogen bonds involving anionic and neutral electron donors, J. Chem. Theory Comput. 9 (11) (2013) 5201–5210.
[27] S. Scheiner, Extrapolation to the complete basis set limit for binding energies of noncovalent interactions, Comput. Theor. Chem. 998 (2012) 9–13.
[28] R. Ditchfield, W.J. Hehre, J.A. Pople, Self-consistent molecular-orbital methods. IX. An extended gaussian-type basis for molecular-orbital studies of organic molecules, J. Chem. Phys. 54 (2) (1971) 724–728.
[29] P.C. Hariharan, J.A. Pople, The influence of polarization functions on molecular orbital hydrogenation energies, Theor. Chim. Acta 28 (3) (1973) 213–222.
[30] T. Clark, J. Chandrasekhar, G.W. Spitznagel, P.V.R. Schleyer, Efficient diffuse function-augmented basis sets for anion calculations. III. The 3–21+G basis set for first-row elements, Li-F, J. Comput. Chem. 4 (3) (1983) 294–301.
[31] J. Gräfenstein, D. Cremer, Efficient density-functional theory integrations by locally augmented radial grids, J. Chem. Phys. 127 (16) (2007) 164113.
[32] V.I. Lebedev, L. Skorokhodov, Quadrature formulas of orders 41, 47 and 53 for the sphere, Russian Acad. Sci. Dokl. Math. 45 (1992) 587–592.
[33] A.E. Reed, L.A. Curtiss, F. Weinhold, Intermolecular interactions from a natural bond orbital, donor-acceptor viewpoint, Chem. Rev. 88 (6) (1988) 899–926.
[34] F. Weinhold, C.R. Landis, Valency and Bonding: A Natural Bond Orbital Donor-Acceptor Perspective, Cambridge University Press, 2005.
[35] R.F.W. Bader, Atoms in Molecules: A Quantum Theory, Oxford University Press, Oxford, 1994.
[36] T.A. Keith, TK Gristmill Software (aim.tkgristmill.com, Overland Park, KS, USA, 2011.
[37] D. Cremer, E. Kraka, A description of the chemical bond in terms of local properties of electron density and energy, Croat. Chem. Acta 57 (6) (1984) 1259–1281.
[38] D. Cremer, E. Kraka, Chemical bonds without bonding electron density - does the difference electron density analysis suffice for a description of the chemical bond?, Agnew Chem. Int. Ed. Engl. 23 (1984) 627–628.
[39] E. Kraka, D. Cremer, Chemical implication of local features of the electron density distribution, in: Z.B. Maksic (Ed.), Theoretical Models of Chemical

Bonding, The Concept of the Chemical Bond, vol. 2, Springer Verlag, Heidelberg, p. 453.
[40] W.H.E. Schwarz, P. Valtazanos, K. Ruedenberg, Electron difference densities and chemical bonding, Theor. Chim. Acta 68 (6) (1985) 471–506.
[41] E. Kraka, W. Zou, M. Filatov, Y. Tao, J. Grafenstein, D. Izotov, J. Gauss, Y. He, A. Wu, Z. Konkoli, V. Polo, L. Olsson, Z. He, D. Cremer, COLOGNE2017, 2017. <http://www.smu.edu/catco>.
[42] M.J. Frisch, G.W. Trucks, H.B. Schlegel, G.E. Scuseria, M.A. Robb, J.R. Cheeseman, G. Scalmani, V. Barone, B. Mennucci, G.A. Petersson, co workers, Gaussian 09 Revision A. 1, Gaussian Inc. , Wallingford, CT, 2010.
[43] T. Lu, F. Chen, Multiwfn: a multifunctional wavefunction analyzer, J. Comput. Chem. 33 (5) (2011) 580–592.
[44] C. Perez, M.T. Muckle, D.P. Zaleski, N.A. Seifert, B. Temelso, G.C. Shields, Z. Kisiel, B.H. Pate, Structures of cage, prism, and book isomers of water hexamer from broadband rotational spectroscopy, Science 336 (6083) (2012) 897–901.
[45] E. Kleinpeter, S. Klod, W.-D. Rudorf, Electronic state of push-pull alkenes: an experimental dynamic NMR and theoretical ab initio MO study, J. Organ. Chem. 69 (13) (2004) 4317–4329.
[46] A.E. Reed, F. Weinhold, L.A. Curtiss, D.J. Pochatko, Natural bond orbital analysis of molecular interactions: theoretical studies of binary complexes of HF, H_2O, NH_3, N_2, O_2, F_2, CO, and CO_2 with HF, H_2O, and NH_3, J. Chem. Phys. 84 (10) (1986) 5687–5705.
[47] S.J. Grabowski, What is the covalency of hydrogen bonding?, Chem Rev. 111 (4) (2011) 2597–2625.
[48] F. Weinhold, R.A. Klein, What is a hydrogen bond? Mutually consistent theoretical and experimental criteria for characterizing h-bonding interactions, Mol. Phys. 110 (9–10) (2012) 565–579.
[49] F. Weinhold, R.A. Klein, Anti-electrostatic hydrogen bonds, Angew. Chem. Int. Ed. 53 (42) (2014) 11214–11217.
[50] A.J. Stone, Natural bond orbitals and the nature of the hydrogen bond, J. Phys. Chem. A 121 (7) (2017) 1531–1534.